# EXCLUSIVE DILEPTON PRODUCTION IN ULTRAPERIPHERAL LEAD–LEAD COLLISIONS IN THE ATLAS EXPERIMENT* **

Agnieszka Ogrodnik

on behalf of the ATLAS Collaboration

AGH University of Science and Technology
Faculty of Physics and Applied Computer Science
al. Mickiewicza 30, 30-059 Kraków, Poland

*(Received March 26, 2021; accepted May 4, 2021)*

Exclusive dilepton pairs are produced via electromagnetic interactions in ultraperipheral heavy-ion collisions (UPC). Electromagnetic fields associated with relativistic lead nuclei can be considered as fluxes of quasi-real photons. The dilepton photoproduction, $\gamma\gamma \to \ell^+\ell^-$, is one of the fundamental processes in UPC and, therefore, can provide a reference for other processes. Given the large theoretical uncertainty of photon flux modelling, its precise measurement with exclusive dilepton pairs can improve predictions for other photoproduction processes. The results for the $\gamma\gamma \to \mu^+\mu^-$ process using 2015 Pb+Pb data collected by the ATLAS experiment at the Large Hadron Collider are presented along with control distributions for the $\gamma\gamma \to e^+e^-$ process in 2018 Pb+Pb data.

DOI:10.5506/APhysPolB.52.1039

## 1. Introduction

Apart from the main proton–proton (*pp*) physics programme, the ATLAS experiment [1] at the Large Hadron Collider (LHC) also collects data from heavy-ion (HI) collisions. Typically, in these events, a major detector activity is observed, due to multiple strong interactions between nucleons. However, in so-called ultraperipheral collisions (UPC), we observe low detector activity and low track multiplicities. The UPC occur when two nuclei

* Presented at XXVII Cracow Epiphany Conference on *Future of Particle Physics*, Cracow, Poland, January 7–10, 2021.

** This work was supported in part by the National Science Centre, Poland (NCN) grants ETIUDA UMO-2020/36/T/ST2/00086 and UMO-2016/23/B/ST2/01409 and by PL-Grid Infrastructure. 

interact with impact parameter larger than twice the radius of the nucleus and electromagnetic (EM) interactions are favoured. The relativistic nuclei are surrounded by large EM fields that can be interpreted as fluxes of photons with small virtuality according to the equivalent photon approximation [2, 3]. The photon–photon luminosities are strongly enhanced in HI collisions with respect to the $pp$ system because each photon flux scales with the $Z^2$ (where $Z$ is the atomic number of the colliding nucleus).

One of the basic processes that can be measured in UPC is exclusive production of dileptons, $\gamma\gamma \to \ell^+\ell^-$, where $\ell^\pm$ stands for $e^\pm$ or $\mu^\pm$. Figure 1 shows the leading-order (LO) Feynmann diagram of the exclusive dimuon photoproduction, $\gamma\gamma \to \mu\mu$, in lead–lead (Pb+Pb) collisions. In this process, the Pb ions stay intact and the final state consist of only two muons. This means a very clean experimental signature that also gives a possibility to study properties of the initial state. As a fundamental process, exclusive dilepton production can provide a reference for measurements of rare processes induced by photons. Thanks to studies of the initial state, it could provide a valuable reference for theoretical approaches in modelling of the initial-photon fluxes.

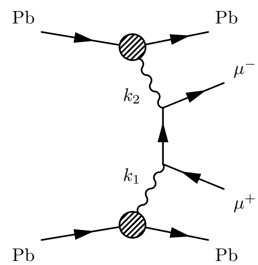


Fig. 1. Leading-order Feynmann diagram of exclusive dimuon photoproduction [7].

## 2. Exclusive dimuon production in 2015 Pb+Pb data

Exclusive dimuon production has been measured by the ATLAS experiment based on 0.48 nb$^{-1}$ of Pb+Pb collision data at $\sqrt{s_{NN}} = 5.02$ TeV collected in 2015. The final-state muons have low transverse momentum, $p_{\mathrm{T}}$, and are produced back-to-back in the azimuthal angle. It is reflected in the definition of the fiducial region of the measurement. Only events with two muons having $p_{\mathrm{T}} > 4$ GeV and $|\eta| < 2.4$ are selected. These requirements are determined by the threshold and acceptance of the muon trigger. Additionally, the dimuon mass, $m_{\mu\mu}$, has to be larger than 10 GeV to avoid contamination of the sample by background dimuons originating from decays of low-mass particles. Finally, $p_{\mathrm{T}}$ of the dimuon system, $p_{\mathrm{T}}^{\mu\mu}$, has to be below 2 GeV, what reflects a back-to-back topology. After the full event selection, the irreducible background from events with nucleus dissociation remains. These background events occur when one of the incoming nuclei dissociates (single dissociation) and a photon is emitted by the substructure of the nucleon. The double dissociation, when both nuclei break up, is also possible.

The selected events are compared with the Monte Carlo predictions of the signal process using STARlight [4] generator (for the LO) or STARlight interfaced to PYTHIA 8 [5] generator (for the next-to-leading order process, *e.g.* final-state radiation, FSR). The dissociative background is simulated with LPAIR [6] generator for *pp* collisions and normalised using data.

Selected events can be divided into 3 categories depending on their activity in the forward direction. In the ATLAS detector, this is described using the information from the Zero-Degree Calorimeters (ZDC). It is installed at a distance of $\pm 140$ m from the interaction point in the vicinity of the beam pipe. The purpose of the ZDC is to detect forward, *i.e.* having $|\eta| > 8.3$, neutrons in HI collisions. In the dilepton events, when there is no nuclear breakup, the signal on both sides of the ZDC should be consistent with zero neutrons (marked as a 0n0n topology). For the background events, one can expect a signal in the ZDC on one (single dissociation, 0nXn) or both (double dissociation, XnXn) sides of the detector. There are also independent processes that result in the increased activity in the ZDC, which are the presence of EM pile-up or possible nucleus excitation followed by neutron emission. Due to these processes, events migrate from the 0n0n category (at the moment of interaction) to 0nXn and XnXn categories (at the detector level), or from the 0nXn to the XnXn category. Therefore, the background contribution cannot be removed and is estimated using a data-driven technique. The correlation of the ZDC signals from the two directions is presented in Fig. 2. The dominant contribution is from the 0n0n category, what corresponds to a peak around 0. The second most likely configuration is an

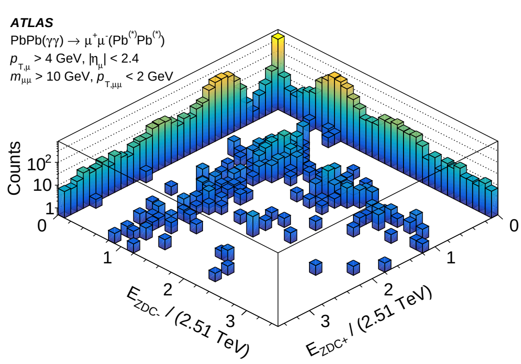


Fig. 2. Correlation of the distributions of ZDC energies in selected events, normalised by the beam energy per-nucleon of 2.51 TeV [7].

observation of one or more neutrons in only one of the ZDC sides (0nXn). The least probable configuration is observing neutron signal on both sides of the ZDC.

The fractions of background events are expected to vary depending on the dimuon mass and rapidity. Therefore, the dimuon kinematics are split into three bins in $m_{\mu\mu}$ (with boundaries at 10, 20, 40 and 80 GeV) and three bins in $|y_{\mu\mu}|$ (with boundaries at 0, 0.8, 1.6 and 2.4). The differences between ZDC topology categories are also visible in acoplanarity $\alpha = 1 - |\Delta\phi|/\pi$ distribution. The signal events exhibit a strong peak at 0 with a tail populated by dimuon events with FSR. The background events are distributed more uniformly in acoplanarity, the distribution is slowly dropping from the highest value at 0, creating a long tail. For each kinematic selection (bins in $m_{\mu\mu}$ and $|y_{\mu\mu}|$), the simultaneous fit is performed in all ZDC topology classes to estimate a fraction of dissociative events, $f_{\mathrm{dis}}$.

Using the estimated fraction of background events, the differential cross section for signal as a function of dimuon kinematic variable, $X_{\mu\mu}$, is measured using the following formula:

$$\frac{\mathrm{d}\sigma_{\mu\mu}}{\mathrm{d}X_{\mu\mu}} = \frac{C_{\mathrm{mig}}}{\mathcal{L}_{\mathrm{int}}} \sum_{\mathrm{events}} \frac{(1 - f_{\mathrm{dis}})}{\varepsilon_{\mathrm{R}_{\mu\mu}} \varepsilon_{\mathrm{T}_{\mu\mu}}} ,$$

where $C_{\mathrm{mig}}$ is a bin migration factor at the $p_{\mathrm{T}} = 4$ GeV boundary, $\mathcal{L}_{\mathrm{int}}$ is integrated luminosity of the Pb+Pb data set, $\varepsilon_{\mathrm{R}_{\mu\mu}}$ and $\varepsilon_{\mathrm{T}_{\mu\mu}}$ are reconstruction and trigger efficiencies, respectively. The first efficiency is determined per one muon with dedicated single muon Monte Carlo (MC) samples using a tag-and-probe method. The trigger efficiency is determined using minimum-bias data and varies in the 93–97% range depending on $m_{\mu\mu}$ and $|y_{\mu\mu}|$. The bin migration factor is estimated in each kinematic variable using signal events simulated with STARlight. Figure 3 presents the differential cross section for exclusive dimuon production as a function of $|y_{\mu\mu}|$ in three mass slices compared with the STARlight prediction for the signal process. The data-to-simulation ratio shows good agreement for central rapidities but it increases with higher $|y_{\mu\mu}|$.

The muon kinematics can also be used to estimate initial-photon energies, $k_{\mathrm{min,\,max}}$, as

$$k_{\mathrm{min,\,max}} = (1/2) m_{\mu\mu} \exp(\pm y_{\mu\mu}) .$$

Figure 4 shows the differential cross section, presented as a function of maximum and minimum photon energies and compared with the STARlight calculations. The predictions are in agreement with data in the intermediate region 5–20 GeV, but they fail to describe the data for lower $k_{\mathrm{min}}$ and higher $k_{\mathrm{max}}$. This suggests that there is a need for refinement of the initial-photon spectrum used in the simulation, which may improve the data-to-prediction comparison.

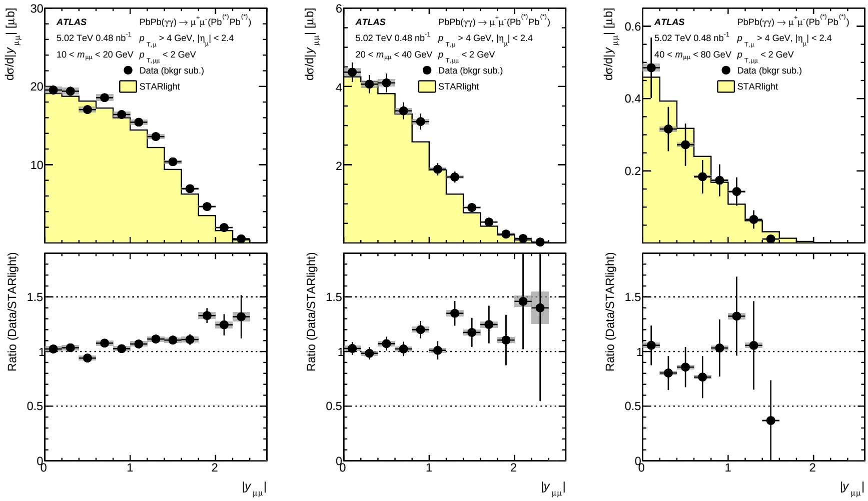


Fig. 3. Differential cross section for exclusive dimuon production in UPC Pb+Pb data as a function of $|y_{\mu\mu}|$ for events passing fiducial acceptance requirements in three mass slices [7].

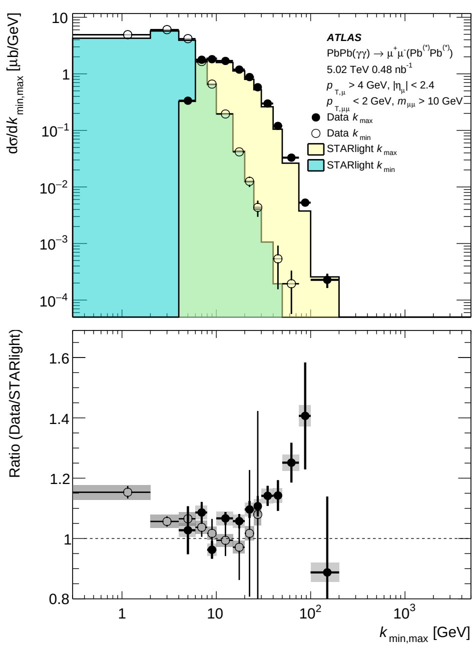


Fig. 4. Differential cross section for exclusive dimuon production in UPC Pb+Pb data as a function of $k_{\mathrm{min,\,max}}$ for events passing fiducial acceptance requirements compared to cross sections from STARlight [7].

## 3. First look at dielectron pairs in 2018 Pb+Pb data

Experimentally, the dielectron photoproduction is a more challenging process than dimuons due to less efficient techniques to trigger on and reconstruct these low energy particles. In 2018 Pb+Pb data taking, a trigger strategy to detect dielectron pairs has been optimised, especially at the Level-1 trigger, with respect to 2015. The resulting efficiency is presented in Fig. 5 as a function of the sum of two calorimeter clusters associated with electron candidates. A significant improvement in efficiency in the low-energy region is visible. This allows to use a lower $p_{\mathrm{T}}$ requirement on a single electron than it was used in the dimuon analysis. Additionally, the integrated luminosity of the 2018 dataset is about 3.5 times larger than the 2015 dataset, what will result in a better statistical precision of the measurements.

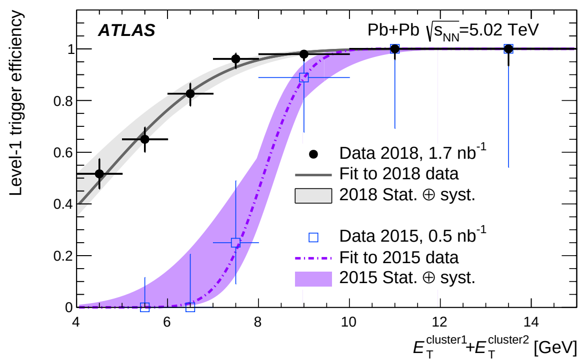


Fig. 5. Efficiency of the Level-1 trigger for dielectron events as a function of the sum of two calorimeter clusters associated to electron candidates [8].

The dielectron pairs were used for performance studies in light-by-light scattering measurement [8] using the 2018 Pb+Pb data. The $e^+e^-$ event candidate should pass the dielectron trigger and several requirements: exactly two oppositely charged electrons with $p_{\mathrm{T}} > 2.5$ GeV, $|\eta| < 2.47$ (excluding $1.37 < |\eta| < 1.52$, where calorimeter resolution is low), veto on additional tracks (only two from electrons are accepted), and dielectron acoplanarity below 0.01. Selected data were compared with the STARlight simulation of the dielectron production in $m_{ee}$ and $p_{\mathrm{T}}^{ee}$ distributions in Fig. 6. In general, good agreement is found between data and simulation. The disagreement in the tail of the $p_{\mathrm{T}}^{ee}$ distribution is likely due to the lack of the FSR effect in the pure STARlight sample.

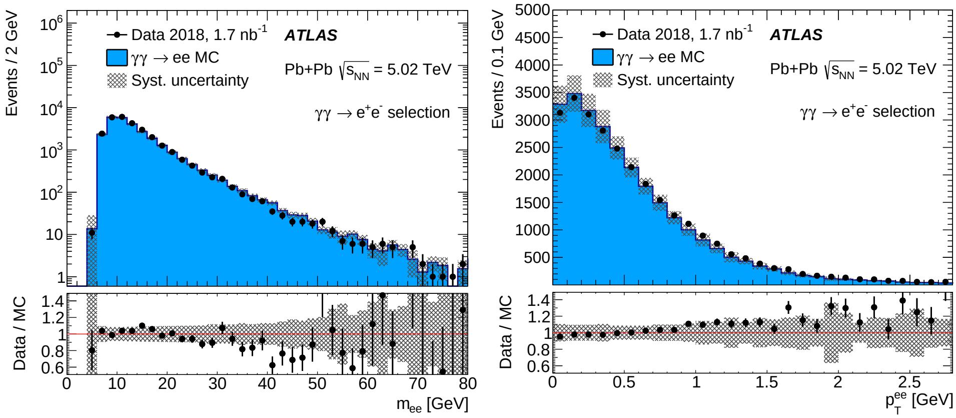


Fig. 6. Kinematic distributions for $\gamma\gamma \to e^+e^-$ event candidates: dielectron invariant mass (left) and dielectron $p_{\mathrm{T}}$ (right) [8]. Data (points) are compared to MC predictions (histograms). The statistical uncertainties on the data are shown as vertical bars, while the systematic uncertainties are represented as the shaded bands. The bottom panels present the data-to-simulation ratio.

## 4. Summary

The ATLAS experiment at the LHC performed a measurement of the dimuon photoproduction using the Pb+Pb collision data recorded in 2015. The results are a reference for various theoretical approaches to model the exclusive dilepton production. The Pb+Pb data collected in 2018 can be used to perform a precise measurement of the dielectron photoproduction.

## REFERENCES


[1] ATLAS Collaboration (G. Aad *et al.*), «The ATLAS Experiment at the CERN Large Hadron Collider», *JINST* **3**, S08003 (2008).

[2] E. Fermi, «Sulla teoria dell' urto tra atomi e corpuscoli elettrici», *Nuovo Cim.* **2**, 143 (1925), arXiv:hep-th/0205086.

[3] E.J. Williams, «Nature of the High Energy Particles of Penetrating Radiation and Status of Ionization and Radiation Formulae», *Phys. Rev.* **45**, 729 (1934).

[4] S.R. Klein *et al.*, «STARlight: A Monte Carlo simulation program for ultra-peripheral collisions of relativistic ions», *Comput. Phys. Commun.* **212**, 258 (2017).

[5] T. Sjöstrand *et al.*, «An introduction to PYTHIA 8.2», *Comput. Phys. Commun.* **191**, 159 (2015).

[6] J.A.M. Vermaseren, «Two-photon processes at very high energies», *Nucl. Phys. B* **229**, 347 (1983).

[7] ATLAS Collaboration, «Exclusive dimuon production in ultraperipheral Pb+Pb collisions at $\sqrt{s_{NN}} = 5.02$ TeV with ATLAS», arXiv:2011.12211 [nucl-ex].

[8] ATLAS Collaboration (G. Aad *et al.*), «Measurement of light-by-light scattering and search for axion-like particles with 2.2 nb$^{-1}$ of Pb+Pb data with the ATLAS detector», *J. High Energy Phys.* **2103**, 243 (2021), arXiv:2008.05355 [hep-ex].